

Distributions of sediments of the tidal flats in response to dynamic actions, Yangtze (Changjiang) Estuary

YAN Hong^{1,2}, *DAI Zhijun¹, LI Jiufa¹, ZHAO Jianchun¹, ZHANG Xiaoling¹, ZHAO Junkai¹

1. State Key Laboratory of Estuarine and Coastal Research, East China Normal University, Shanghai 200062, China;

2. Faculty of Civil Engineering and Geosciences, Delft Technical University, Delft 2600, the Netherlands

Abstract: Sediment samples with high spatial resolution (432 samples in total) and flow data were collected on the tidal flats in the mouth-bar region of the Yangtze Estuary. The data was collected in July 2005, July 2006 and May 2007. The samples were analyzed with a particle sizer, resulting in the sediment distribution. The grain sizes and related parameters were analyzed. The results were presented in a ternary diagram. The sediment mainly consisted of sand, silty sand, sandy silt, sand-silt-clay, silt and clayey silt. And sand skeletons and clay matrices were found. At Nanhui Shoal, silt skeletons could be identified as well. Furthermore, the results were discussed per shoal. Although some depth dependencies were found per shoal, no general relation was found. The results are as follows: sediment located at these tidal flats of the Yangtze Estuary was mainly composed of sand, silty sand and silt. The median grain size in sediment was relatively complex with a range from 2.5 ϕ to 8 ϕ . The distributions of sorting coefficients ranging from 1 to 2 were in agreement with median sizes. It was suggested that sediment of the tidal flats was coarser and better sorted or finer and worse sorted. The skewness in sediment distribution varied from 0.1 to 0.8. In addition, the distributions of sorting coefficient and skewness in sediment at Chongming Eastern Shoal, Hengsha Eastern Shoal and Jiudian Shoal were of similar characteristics because there were closely positive correlated relationships among these parameters. However, due to the location difference between Nanhui Southern Shoal and Eastern Shoal, the values of sorting coefficient and skewness had relatively large distinctions. The tracks of sediment transport could be described based on the distributions of sediment, which might reveal sediment transport controlled by two dominant hydrodynamic factors of current and wave. It was appreciable that coarser sediment with lower sorted coefficient was affected by dominant ebb current action and intense wave action resulted from rapidly dissipated wave energy. Moreover, due to the effects of obstructed branches, guided current and broken wave actions of the Deep Water Channel Project, grain-size in sediment located at two sides of the groyne was of uneven distribution characteristics.

Keywords: sediment; tidal flat; deposition; wave action; tidal current; Yangtze (Changjiang) Estuary

Received: 2010-04-19 **Accepted:** 2010-06-30

Foundation: Key Project for the National Natural Science Foundation of China, No.50939003; National Natural Science Foundation of China, No.40976055; No.41076050

Author: Yan Hong (1984–), Ph.D, specialized in estuarine and coastal morphodynamics. E-mail: hong.yan@tudelft.nl

***Corresponding author:** Dai Zhijun, Professor, E-mail: zjdai@sklec.ecnu.edu.cn

1 Introduction

The shoals in the Yangtze Estuary are important for a variety of functions. For example, they are and have been used for land reclamation; they form important ecological areas; and they play a role in safety by reducing wave heights. In the past two thousand years, large parts of the tidal flats have been reclaimed. 62% of land area in Shanghai is reclaimed tidal flat (Li *et al.*, 2007). Chongming Eastern Shoal and Jiuduan Shoal are currently protected as national nature and wetland reserves. The estuary is, however, subject of changes by nature and anthropogenic activities. The sediment load from the Yangtze River has been intensely changed by increasing human interferences (e.g. the constructions of Three Gorges Reservoir located at the upstream site of the Yangtze River); sea level rise impacts the morphological system over long time scales; construction works, like the Deep Water Channel Project, change the hydrodynamics and sediment transport (Wan *et al.*, 2003; Fu *et al.*, 2003; Shen *et al.*, 2000; Yoshiki *et al.*, 2001). To understand the response of the estuary to the human interventions, it is of importance to understand the sediment processes in the estuary. The spatial and temporal distribution of the estuarine tidal flat sediment in the Yangtze Estuary is impacted by the complex interaction of river runoff, tides and waves (Li *et al.*, 1988; Dai *et al.*, 2011). Measuring the sediment distribution therefore tells something about the sediment transport processes, although there is still no unified theory (Hartmann, 2007). In this paper a new data set of sediment samples of the shoals in the Yangtze Estuary is presented (Figure 1). The Chinese version was published in Yan *et al.* (2009). Sediment samples were obtained on a large scale and with a high resolution from subtidal areas of Chongming Eastern Shoal, Hengsha Eastern Shoal, Jiuduan Shoal and Nanhui Shoal. The particle-size distributions (PSD) of these tidal flats were analyzed. The aim of this paper is to present the data and to interpret them in order to understand the sediment processes on the subtidal areas of the main shoals in the Yangtze Estuary.

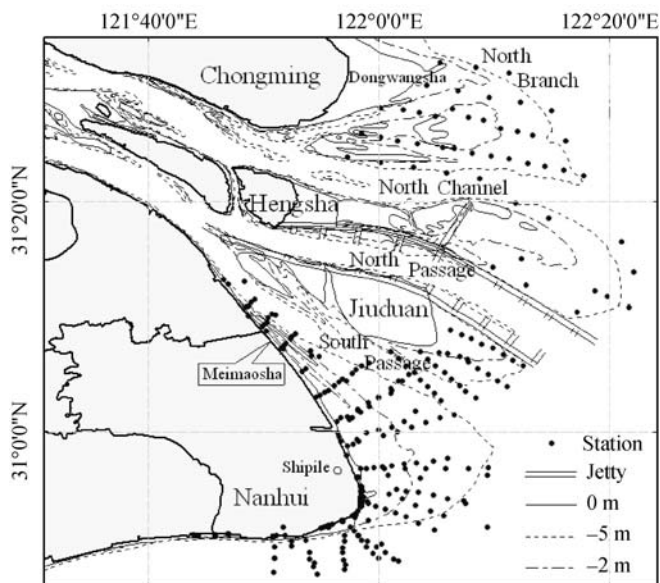


Figure 1 The sketch of study area and sample stations

2 Study areas

The Yangtze Estuary is one of the typical braided-type estuaries, and its morphodynamic patterns from Xuliujing to the mouth can be described as “three-order bifurcations and four-outlet diversions into the sea.” Meanwhile, the Yangtze Estuary is a meso-tidal estuary with average tidal ranges from 2.4 to 3.2 m. It can be seen that there are four tidal flats located in the Yangtze Estuary (Figure 1). These tidal flats are named as Chongming Eastern Shoal, Hengsha Eastern Shoal, Jiuduan Shoal and Nanhui Shoal from north to south of the Yangtze Estuary, respectively, which can be mainly parts of the typical shoal and channel systems formed by the various dynamical interactions between land and sea (Chen, 2007). Chongming Eastern Shoal, located at the site of between the North Branch and North Channel, is a kind of shadow island shoal. Hengsha Eastern Shoal, located at the tail of Hengsha Island, is composed of Hengsha Eastern Shoal, Hengsha lower tidal shoals and their sub-tidal flats with a total area of 503 km². The north jetty of Deepwater Channel Regulation Projection was built at the south side of Hengsha shoal. Jiuduan Shoal, located at the area of between North Channel and North Passage, has a total area of 419 km². Nanhui Shoal, located at the junction of South Channel and land, is a kind of edge-typed spits, which can be divided into two parts: Eastern Shoal and Southern Shoal.

In the estuarine area, the frequent changes of water depth on tidal flat in time and space formed a unique hydrodynamic environment of tidal flat which controls sediment transport processes. It can be testified that there are two main hydrodynamic factors for tidal flats: tidal currents and waves (Roberts *et al.*, 2000). Tidal currents vary in a regular way and waves change in a random way (Green *et al.*, 1997). In channels and subtidal flats, the peak flow velocity is approximate 2 m/s during spring tides. Near the river mouth, mean and maximum wave heights are 1.0 and 6.2 m (at Zhongjun Ship Gauging Station near the river mouth) with an upstream decreasing trend (CCSA, 1997). Flow measurements were carried out within the same project. These are however not discussed in detail here; see Chen (2003) and Fu (2007) for more details.

3 Materials and methods

A total of 432 surface sediment samples were taken at the four tidal flats of the Yangtze Estuary. They were taken by means of a grab (clamshell) sampler. The samples were taken at different periods: Chongming, Hengsha and Jiudan in May 2007, and Nanhui in July 2005 and July 2006. This implies that the measurements were carried out during the flood season with comparatively hydrodynamic and suspended sediment concentration. We consider the subtidal shoal only, where vegetation is not dominating. So, we restrict ourselves to the region with a water depth ranging from 0 m till ca 5 m. The exact locations of the samples were determined by the global positioning system (GPS); see Figure 1. Particle-size distributions (PSD) were determined in the laboratory, using a LS-100 particle size analyzer, after sodium hexametaphosphate solution and ultrasonic dispersion. Based on these distributions, statistical values like the median size, sorting coefficient and skewness were defined.

Furthermore, the samples were classified in a sand-silt-clay diagram, based on the different percentage of sand, silt and clay by dry weight. Different sub-divisions of the triangle are proposed, e.g. by Shepard (1953) or Flemming (2000). However, these subdivisions have a

weak physical basis. Van Ledden (2003) proposed a physically based subdivision. A first division is made between cohesive and non-cohesive sediment, based on the clay content, resulting in a horizontal line in the triangle. A critical value of 7% is used by Van Ledden (2003). Furthermore, a division is made between a grain skeleton and a mud matrix. As we make a distinction between sand and silt, two lines are required, one between the mud matrix and the sand skeleton (left side of the triangle) and one between the mud matrix and the silt skeleton (on the right side). These division lines are dependent on the water content and on the minimum volume content of sand (silt) to form a sand (silt) skeleton. This minimum volume content is set to 40% (Van Ledden, 2003). Different values for the water content are given, ranging from 40% till 50%. Based on these division lines, six areas are found: I non-cohesive sand; II cohesive sand; III non-cohesive mixed; IV cohesive clay; V non-cohesive silt; and VI cohesive silt. The regions are given in Figure 2. Note that the used axes of the ternary diagram (following Van Ledden, 2003) are different from the ones of Flemming (2000). The locations of the samples in the diagrams is however the same.

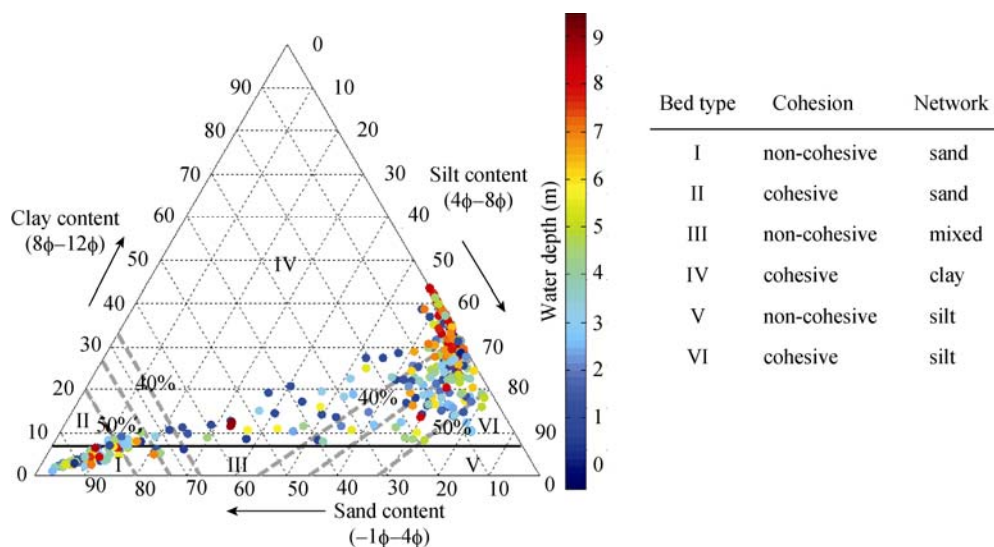


Figure 2 Sand-silt-clay triangular diagram in sediments

4 Components and PSD characteristics in surficial sediments

Analysis of PSD can help in evaluating sediment transport, deposition and size-selective erosion; see Dai *et al.* (2010). However, there is still a debate about the understanding of sedimentary processes by means of PSD (Hartmann, 2007). In this section, we first describe the results of all data by means of the ternary diagram. Secondly, the sediment samples are discussed for each shoal individually.

All sediment samples are classified, and plotted in the sand-silt-clay diagram (Figure 2). Based on the classification of Shepard (1953), six primary sediment types can be found in the Yangtze Estuary including sand, silty sand, sandy silt, sand-silt-clay, silt and clayey silt. Based on the classification of Van Ledden (2003), we see two types of sediment beds: non-cohesive beds with a sandy skeleton (Type I) and cohesive beds with a clay water matrix (Type IV). Only at Nanhui shoal, a cohesive bed with a silt skeleton (Type VI) could be

identified, depending on the water content. A clear decision could not be given as the water content was not measured. Apparently, silt skeletons (Type V and VI) are not present. The energetic environment could be a possible explanation. Loosely packed silt skeletons have a low critical shear stress, and can therefore hardly persist. Higher critical shear stresses can be found for: (1) A denser packing (lower water content). In that case, the division line between Type IV and Type V/VI shifts to the lower right corner. It is known that densely packed silt beds can have very high critical shear stresses (Winterwerp and Van Kesteren, 2004). (2) A higher clay content (more cohesion). The position in the diagram shifts upwards (and somewhat leftwards). (3) Larger grain sizes. The position of the sample in the diagram shifts leftwards. Single grains are than more stable. A similar analysis can be made for the mixed sediment. Cohesionless mixtures (Type III) do not exist as the critical shear stress of such mixtures is low.

The types I and IV can have relatively high critical shear stresses: Type I because of large grains and Type IV because of strong cohesion. It is therefore likely that these types dominate, as the hydrodynamic forces are relatively strong on the subtidal shoals.

No samples are also found with ratios clay/silt > 0.67 . As mentioned by Flemming (2000), many estuaries have a close to constant ratio between clay and silt. The value can however differ. The samples in the Yangtze Estuary also show a band with a ratio of clay/silt ≈ 0.4 . No sound physical evidence is known for such constant ratios. Winterwerp and Van Kesteren (2004) explain it by entrapment of the silt particles by clay particles. A link with the sediment distribution from the incoming sediment from the river is also likely.

The current roses in Figure 7 indicate that high velocities are found at deep water and low velocities at shallow water, as would be expected for friction dominated flow. Consequently, a dependency of the bed level would be expected on the sediment distribution. Therefore, the bed level is indicated in Figure 2 as color. However, no relationship is found. One of the counter-acting mechanisms is the impact of waves. Waves are more effective on shallow water than in deep water. No relation between sediment distribution and water depth could be interpreted as an influence of currents and waves. The spatial distribution is discussed in more detail in the next section.

4.1 Sediment components and PSD types of Chongming Eastern Shoal

The surface sediment at Chongming Eastern Shoal could mainly be classified as sand, silty sand, sandy silt, sand-silt-clay, silt and clayey silt, of which sand, sandy silt and clayey silt were dominant. At the Chongming shoal, the flood flow diverges into the North Branch and North Passage. During the ebb, the flow converges. Sandy sediment was found at the eastern tip of the shoal and at the southern part, adjacent to the North Passage. Silty sediment was found closer to the land and on the north side, adjacent to the North Branch. The 2 m contour was roughly the division between clayey-silt sediment and sandy sediment (Figure 3).

Table 1 shows the statistical parameters of the sediment along the transverse section of Chongming Eastern Shoal. It can be seen that the values of median sizes in sediment of Chongming Eastern Shoal were ranged from 8 ϕ (0.004 mm) to 2.5 ϕ (0.177 mm). The median values larger than 7 ϕ were mainly distributed in the area with a depth below 2 m (e.g. Q19, Q20). The samples with median values below 3 ϕ were mainly distributed in the area with a depth over 2 m (e.g. Q24, Q25 and Q30).

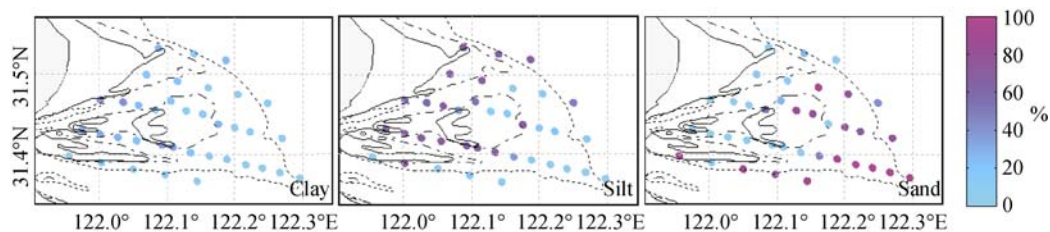


Figure 3 Percentage of the changes of different compositions in surficial sediments of the Chongming Eastern Shoal

Table 1 Characteristics of grain size and classifications in sediments along the transverse section of Chongming Eastern Shoal

Station	Median size (ϕ)	Sorting coefficient	Skewness	Components (%)			Sediment type
				Clay	Silt	Sand	
Q19	7.50	1.81	0.21	39.93	60.03	0.04	Clayey silt
Q20	7.60	1.78	0.20	41.44	58.56	0	Clayey silt
Q21	6.22	2.03	0.22	24.15	68.96	6.89	Clayey silt
Q22	3.90	1.74	0.66	8.57	37.52	53.91	Silty sand
Q24	2.95	1.63	0.75	7.33	11.02	81.65	sand
Q25	2.93	2.03	0.79	9.31	12.35	78.34	sand
Q26	6.73	1.88	0.18	27.94	71.4	0.66	Clayey silt
Q27	3.03	1.83	0.76	7.32	14.51	78.17	sand
Q28	3.47	1.87	0.77	9.41	18.86	71.73	sand

The sorting coefficients ranged from 1.6 to 2.0 along the transverse segment, and reached a maximum value of 2.03 around the area with the depth of 2 m (e.g. Q21, Q25). These relatively high values indicate that the sediment was badly sorted. A clear spatial trend in the sorting coefficient was not found. The skewness was highly correlated with the median diameter. Sandy sediments have higher skewnesses (ca 0.7) than finer sediments (ca. 0.2). Consequently, the skewness increased from west till east on the Chongming Eastern Shoal.

4.2 Components and PSD types along Hengsha Eastern Shoal

Compared to the other tidal flats, sediment in Hengsha Eastern Shoal were generally coarse. In the northeastern part, the sediment was classified as sand and silty sand. Finer sediment was found at the southwestern part of the shoal adjacent to the northern groyne of the North Passage; see Figure 4. No clear dependency between sediment type and water depth was found. This was partly caused by the lack of data in the shallow (<2 m deep) area.

The median sizes of the surface sediment of Hengsha Eastern Shoal were relatively high, with values ranging from 6.5 ϕ to 2.5 ϕ . The sediment near the northern groyne of the North Passage was relatively fine with median sizes of over 6 ϕ . However, coarser sediment with median sizes ranging from 2 ϕ to 3 ϕ was found on the northeast part of Hengsha shoal.

On most parts of the shoal, the sediment was well sorted (1.2–1.5; see Table 2). However, close to the groyne, the sorting coefficient was higher. The groyne along the Deep Water Channel had reduced the flow in northeastern and southwestern direction, resulting in sedimentation of finer material, with a high sorting coefficient, north of the groyne. Moreover,

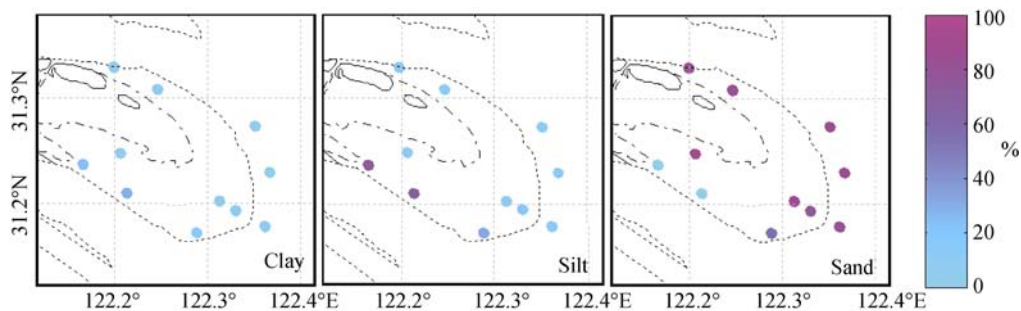


Figure 4 Percentage changes of different compositions in surficial sediments of Hengsha Eastern Shoal

Table 2 Characteristics of grain size and classification in sediments along the transverse section of Hengsha Shallow Shoal

Station	Median size (ϕ)	Sorting coefficient	Skewness	Components (%)			Sediment type
				Clay	Silt	Sand	
H23	6.41	1.83	0.27	24.47	74.78	0.75	Clayey silt
H28	3.57	1.46	0.32	11.81	32.81	55.38	Silty clay
H03	3.05	1.30	0.53	5.12	12.10	82.77	Sand
H07	2.81	1.20	0.50	4.58	8.51	86.91	Sand

particle-size distributions revealed positive skewness with relatively low values between 0.3 and 0.5.

4.3 Components and PSD types on submarine flats of Jiudian Shoal

Figure 5 shows the sediment distribution of Jiudian Shoal. Similar to Chongming Eastern Island, the 2 m contour seems a division line between sandy and silty sediment. However, at Jiudian Shoal the sandy sediment was found for water depths smaller than 2 m, whereas at Chongming Eastern Shoal the sandy sediment was found for water depths larger than 2 m. Silty sediment was found on the southern part of the Jiudian Shoal for water depths larger than 2 m.

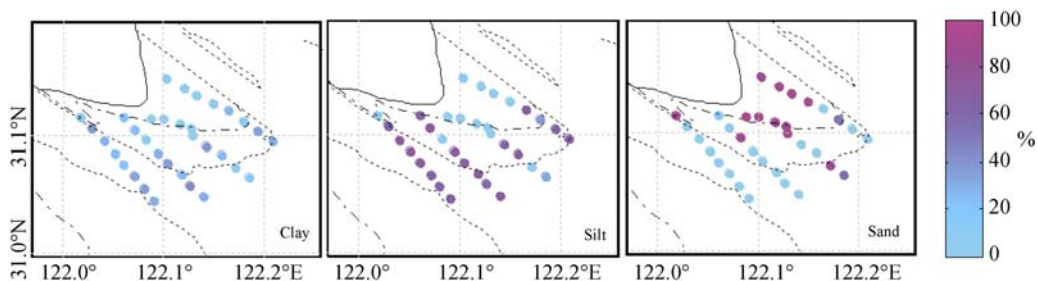


Figure 5 Percentage changes of different compositions in surficial sediments of Jiudian Island

The median sizes at Jiudian Shoal ranged from 7.5 ϕ to 2.5 ϕ (Table 3), and corresponding compositions varied from sand via silty clay to sand along the transverse profile from 0 m contour to 5 m contour. The other transects showed siltier sediment in the deeper areas (>5 m). It is unclear whether the last two samples were local patches of sand.

Table 3 Characteristics of grain size and classification in sediments along the transverse section of Jiudian Shoal

Station	Median size (ϕ)	Sorting coefficient	Skewness	Components (%)			Sediment type
				Clay	Silt	Clay	
J09	2.57	0.97	0.41	3.11	4.96	91.93	Sand
J10	2.55	1.02	0.41	3.18	5.08	91.74	Sand
J11	2.54	1.04	0.45	3.38	6.17	90.45	Sand
J33	2.55	1.24	0.52	4.27	9.08	86.65	Sand
J12	2.52	0.94	0.39	2.71	5.44	91.85	Sand
J13	7.45	1.72	0.12	38.32	61.68	0	Clayey silt
J14	6.63	1.93	0.2	28.11	70.12	1.77	Clayey silt
J15	2.58	1.29	0.67	6.49	8.49	85.02	Sand
J16	3.25	2.27	0.78	12.53	32.53	54.93	Silty sand

A dependency between sorting coefficients and median sizes was found, such that coarse particles generally have better sorting features. The skewness values were around 0.4–0.5 from Station J09 to J12, and around 0.1–0.2 from Station J13 to J14. In conclusion, the PSD features at Jiudian were comparatively related to water depth.

4.4 Components and PSDs types on submarine flats of Nanhui Shoal

Nanhui Shoal is located at the area of hyperconcentration with ample sediment supply from the Yangtze River and from the sea during flood. Compared to the other three shoals, sediment was generally fine, basically dominated by silty sediment. Sandy sediment was found only around the protruded part to the 2 m contour at the junction of the Eastern Shoal and the Southern Shoal. Although the water depths at the southern part were much larger than at the eastern shoal, the difference in sediment distribution was small. The clay content in the southern shoal was higher.

Two transects are shown in Figure 6, one is a typical transect at the eastern shoal with silty sediment, and another at the transitional position between the eastern and the southern shoal with mainly sandy sediment. The median sizes ranged from 2.5 ϕ to 7.6 ϕ (Table 4).

The sorting coefficients ranged from 1.7 to 2.5 along two transverse segments, and reached a maximum value of 2.5 at the Eastern Shoal near the depth of 2 m (e.g. N11).

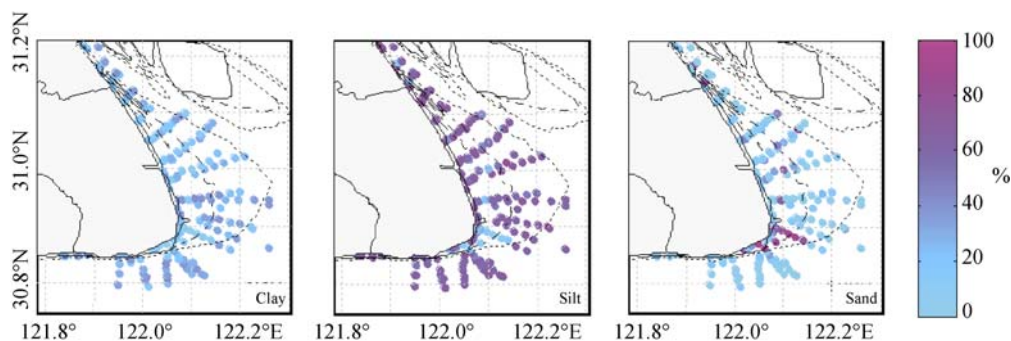
**Figure 6** Percentage of the changes of different compositions in surficial sediments of Nanhui Shoal

Table 4 Characteristics of grain size and classification in sediments along the transverse section of Nanhui Shoal

Station	Median size (ϕ)	Sorting coefficient	Skewness	Components (%)			Sediment type
				Clay	Silt	Clay	
N1	3.49	2.05	0.66	10.66	21.08	68.25	Silty sand
N2	2.65	1.87	0.36	3.08	3.73	93.19	Sand
N3	2.67	1.33	0.55	5.18	8.84	85.98	Sand
N4	2.57	2.33	0.78	10.29	15.7	74.01	Sand
N5	7.12	1.87	0.15	34.52	65.3	0.18	Clayey silt
N6	6.03	2.24	0.21	24.63	62.22	13.15	Clayey silt
N7	7.39	2.05	-0.01	38.76	57.35	3.88	Clayey silt
N8	6.39	2.07	0.23	10.98	89.02	0.00	Silt
N9	7.56	1.73	0.13	35.12	64.69	0.19	Clayey silt
N10	7.14	1.92	0.13	22.70	61.09	16.21	Clayey silt
N11	6.71	2.46	0.17	27.65	67.36	4.99	Clayey silt

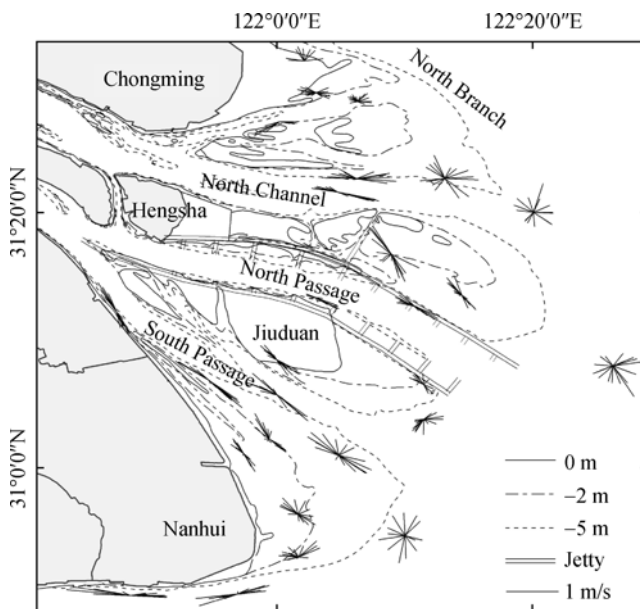


Figure 7 The sketch of current rose of the study area

These relatively high values indicate that the sediment is badly sorted. A clear trend in the sorting coefficient was not found.

5 Sedimentary dynamic processes

Tides and waves are the two forces dominating the sediment dynamics on the tidal flats. Storm surges may also significantly influence the siltation and erosion of tidal flat morphological evolution, although they occurred occasionally (Yang *et al.*, 2001). Wind wave may

be a major dynamical factor in the temporal distribution, because a large amount of bed-load could be re-suspended by uplifted effects of wind waves. Moreover, tidal current processes could be directly impacts on sediment re-suspension transportation, particularly in mouth-bar areas located at the alternation of tidal flats and outlets system. The changes in a local flow field structure due to man-made engineering will cause changes in water flow exchange between shoals and channels. It can promote exchange mechanism between suspended load and bed materials, and can result in uneven distributions in evolution of tidal landforms and sediment. The sediment with poor sorting and positive skewness is often found in shallow coastal areas. The main reasons are: (1) fine-grained sediment itself and the role of the reciprocating moving; (2) Positive skewness reveals there is a wide range of fine particle sizes in PSD, that is mainly influenced by tides current rather than waves. Therefore, the sorting coefficient partly reflects the strength of hydrodynamic conditions in the sedimentary environment; and a difference in skewness, to some extent, reflects different sedimentary processes. The surface sediment at four subtidal flats in the Yangtze Estuary was generally silty or sandy. This situation was coinciding with the local tidal velocity, open frontal waves and other dynamic effects. It was appreciable that coarse sediment with better sorting could be subjected to dominant ebb current and intense wave actions due to rapidly dissipated wave energy.

5.1 Effects of tidal current

The mouth bar areas are mainly characterized by combined effects of open-sea tidal currents and large runoff from the Yangtze River. The current velocity increases in shallow areas with a maximum velocity over 1.3 m (Table 5), which may enhance sediment transport ability and wash away fine bed-load. When the flood tidal currents continue propagating to the middle and high tidal flats, its velocity will decrease because of the effects of terrain resistance. There the maximum velocity of flood and ebb tides are both less than 1.0 m/s, which had suspended-load easy to silt down with fine particles in bed surface. Meanwhile, sediments in shallow water were finer than those in deeper water. This can be explained by the conditions of sediment transportation influenced by the dominant flood current in the areas with the depth of below 2 m, and the dominant ebb current in the area with the depth of over 2 m (Li *et al.*, 1988). Moreover, bed-load at the same depth level in different tidal flats frequently appeared with different PSD due to the Coriolis force as well as local channel flow effects. For example, the further south ebb tide flows in the North Branch carry a large number of suspended sediment into Chongming Eastern Shoal along its north side, and then the suspended sediment trends to deposit under low velocity condition of flow diffusion. That will lead to relatively small particle sizes on the north part of Chongming Eastern Shoal

Table 5 Average values of the measured vertical tidal velocity

Tide	Station	Flood tide			Ebb tide			Altitude (m)
		Mean velocity (cm/s)	Mean direction (°)	Max velocity (cm/s)	Mean velocity (cm/s)	Mean direction (°)	Max velocity (cm/s)	
2006. 7 Spring tide	S1	65	324	94	55	148	86	-1
	S2	62	331	149	71	125	132	-2.5
	S3	105	314	139	106	131	191	-4.5

compared to other places. On the other hand, the sediment of the south part was relatively coarse because of strong effects of further north flood tidal current in the lower North Channel. As a result, sediment of Chongming Eastern Shoal showed a distribution of fine in north and coarse in south. Furthermore, the severe varying dynamical factors in Chongming Eastern Shoal would result in poor sorting features (Li *et al.*, 1988).

Compared to the other three tidal flats, Nanhui Shoal was generally covered by fine surface sediment: about 60% of the area covered by clayey silt. The main reasons can be concluded as: firstly, large amounts of sediment discharge supplied by sufficient suspended sediment source; secondly, the local suspended sediment easily deposited in lowered velocity at this confluent region of the Yangtze Estuary and the north Hangzhou Bay.

5.2 Effect of waves

Wave in the Yangtze Estuary is estimated to start acting effectively at the water depth of 2 m (Zhu *et al.*, 1988). This means that the dynamical erosion and deposition with the depth below 2 m were controlled by seasonal changes of wind waves (Zhu *et al.*, 1988). Fine particles such as silt and clay could be uplifted and moved away during normal waves and then back-deposit with no wave effects, which resulted in a unique sand-silt-clay sediment zone with poor sorting features. In addition, the mean wave effective depth could reach a maximum value of 6 m in some special places such as south Nanhui Shoal, at the mouth of Hangzhou Bay and faced to intense wave action from the East China Sea. In July 2005, this area was mainly impacted by peripheral typhoons of Haitang (0505), Nalgae (0506) and Banyan (0507), with the maximum wind scale of 8–9. Thereby, a large number of coarse sediment could be uplifted to near coastal shoal and then form a large bank of fine sand in the south Nanhui Shoal. That could be the reason why the sediment samples collected in this area were relatively coarse and better sorted.

Based the previous research (Zhang *et al.*, 2002), under extreme weather conditions of typhoons, wave crest will be sharply steepened and wave height will quickly reduce from 4 m to 1 m or so in certain areas such as northwest and southeast of Hengsha Shoal and north of Jiudian Shoal. Sediment samples collected in May 2007 indicates that Typhoon Yutu with a maximum wind speed of 30 m/s had a most active effect on re-suspension of bed-load. During the Typhoon period, sediment was picked up due to waves and then transported up to middle and high tidal flats by tidal currents. This resulted in a distribution of sand with median diameter less than 4ϕ and better sorting. In conclusion, wind waves play an important role during flood season in the distributions of surface sediment and geomorphology, which can explain why Hengsha Shoal is mainly covered by fine sand.

5.3 Effects of Deep Water Channel Project

In addition, due to the effects of the Deep Water Channel Project for obstructing branches, guiding current and breaking waves, the groyne reduced the flow-sediment flux exchanges between Hengsha Eastern Shoal and North Passage. As a result, water level increased on flats and flow velocity decreased in the groyne sheltered segment. Therefore, suspended sediment would have more chance to silt down along the groyne. Meanwhile, the groyne reduces the wave energy from the waves and might contribute to sediment deposition. Moreover, the sediment, carried with tidal current, could easily deposit on both sides of

groynes due to the low velocity there. This resulted in fine sediment at the south Hengsha Eastern Shoal (Du *et al.*, 2007; Yan *et al.*, 2001).

Before the construction of the south groyne, the changes in water-sediment distributions and flow-sediment flux exchanges between North Passage and South Passage often caused alternation of erosion and deposition in lower part of Jiudian Shoal. However, the construction blocked the northwest (around 310°) way of a number of flood channels to North Passage on Jiudian Shoal and changed the flow pattern as well as the pattern of sediment transport. In the changed water and sediment environment, water-sediment exchanges between flats and channels in the south shoal speeded up, resulting in slight siltation and surface sediment refinement (Li *et al.*, 2006). The north Jiudian Shoal, closed to south groyne was mainly affected by returning stroke currents and external wind waves. Therefore, surface sediment of Jiudian Shoal was coarsened by jolt action and retained main components of fine sand and sandy silt with better sorting.

6 Conclusions

(1) The sediment types of the four main subtidal tidal flats in mouth-bar area of the Yangtze Estuary were mainly sand, silty sand, sandy silt, sand-silt-clay, silt, and clayed silt. Among them, sand, silty sand and clayed silt dominated. The water depth contour seems a division line between sandy and silty sediment at Chongming Eastern Shoal and Jiudian Shoal. However, at Chongming Eastern Shoal, sandy sediment is found at the area deeper than 2 m and silty sediment was found at areas shallower than 2 m. At Jiudian, the distribution was apposite: sandy sediment for water depths smaller than 2 m and silty sediment for areas deeper than 2 m. No clear dependency between sediment type and water depth is found at Hengsha Eastern Shoal and Nanhui Shoal.

(2) The values of median sizes varied in space, ranging from 2.5ϕ to 8ϕ . The distribution of sorting coefficients (1–2) was in agreement with median grain sizes. The skewness values varied from 0.1 to 0.8. The distribution values of sorting coefficient and skewness at Chongming Eastern Shoal, Hengsha Eastern Shoal and Jiudian Shoal were of similar characteristics because there were closely positive correlated relationships among these parameters. However, due to the location difference for Nanhui Southern Shoal and Eastern Shoal, these parameters in PSD showed obvious distinctions which reflected complex hydrodynamic actions.

(3) The sediment with poor sorting and positive skewness is found overall the study area. The sorting coefficient may partly reflect the strength of hydrodynamic conditions in sedimentary environment, and skewness, to some extent, may reflect different sedimentary processes. Sediment transportation in our study area is controlled by the two dominant hydrodynamic factors of tidal currents and wave. The geomorphological evolution and non-uniformity of sediment distributions are directly related with water- and sediment exchanges between flat and channel, local tidal current of shoal, open frontal wind waves and artificial constructions in mouth-bar area with shoal topography of channel and flat system.

Acknowledgement

The authors would like to thank Dr. Bram van Prooijen in Delft University of Technology,

for his detailed comments and his help for improving English writing.

References

- CCSA (Compiling Committee of 'Shanghai Atlas'), 1997. Shanghai Atlas. Shanghai: Shanghai Technical Press.
- Chen Jiyu (eds.), 2007. The Research and Practice on Chinese Estuary and Coast. Beijing: Higher Education Press. (in Chinese)
- Chen Shenliang, Zhang Guoan, Gu Guochuan, 2003. Geomorphic evolution fo Nanhui nearshore of the Yangtze Estuary and its sediment dynamic mechanism. *Shanghai Geology*, 2003, (4): 1–4. (in Chinese)
- Chen Shenliang, Zhang Guoan, Yang Shilun *et al.*, 2006. Temporal variations of fine suspended sediment concentration in the Changjiang River estuary and adjacent coastal waters, China. *Journal of Hydrology*, 331: 137–145.
- Chen Z, Li J, Shen H *et al.*, 2001. Changjiang of China: historical analysis of discharge variability and sediment flux. *Geomorphology*, 41: 77–91.
- Dai Zhijun, Chen Jiyu, Cheng Heqin *et al.*, 2005. Sediment characteristics and transport patterns in Nanhui adjacent area. *Resources and Environment in the Yangtze Basin*, 14(6): 735–739. (in Chinese)
- Dai Zhijun, Du Jinzhou, Chu Ao *et al.*, 2010. Sediment characteristics in the North Branch of the Yangtze Estuary based on radioisotope tracers. *Environmental Earth Sciences*, DOI: 10.1007/s12665-010-0647-7.
- Dai Zhijun, Du Jinzhou, Zhang Xiaoling *et al.*, 2011. Variation of riverine material loads and environmental consequences on the Changjiang estuary in recent decades (1955–2008). *Environmental Science and Technology*, 2011, 45: 223–227.
- Du Jinglong, Yang Shilun, 2007. Influence of Deep-Water Channel Project at North Passage of the Yangtze River on erosion and accumulation of Hengsha east shoal and Jiuduansha shoal. *Scientia Geographica Sinica*, 27(3): 390–394. (in Chinese)
- Flemming B W, 2000. A revised textural classification of gravel-free muddy sediments on the basis of ternary diagrams. *Continental Shelf Research*, 20: 1125–1137.
- Folk R L, Ward W C, 1957. Brazos River Bar: A study in the significance of grain size parameters. *Journal of Sedimentary Petrology*, 27: 3–27.
- Fu Gui, Li Jiufa, Ying Ming *et al.*, 2007. Analysis on recent topography evolution of Nanhui tidal flats in Yangtze Estuary. *Marine Science Bulletin*, 2007, (2): 105–112. (in Chinese)
- Fu Renshou, Yu Zhiying, Jin Liu *et al.*, 2003. Variation trend of runoff and sediment load in Yangtze River. *Journal of Hydraulic Engineering*, (11): 21–29. (in Chinese)
- Green M O, Black K P, Amos C L, 1997. Control of estuarine sediment dynamics by interactions between currents and waves at several scales. *Marine Geology*, 144: 97–116.
- Hartmann D, 2007. From particle size to sediment dynamics: An introduction. *Sedimentary Geology*, 202: 333–336.
- Li Jiufa, 1991. The rule of sediment transport on the Nanhui tidal flat in the Changjiang Estuary. *Acta Oceanologica Sinica*, 10(1): 117–127.
- Li Jiufa, Dai Zhijun, Ying Ming *et al.*, 2007. Analysis on the development and evolution of tidal flats and reclamation of land resource along shore of Shanghai city. *Journal of Natural Resources*, 22(3): 361–371. (in Chinese)
- Li Jiufa, Mao Zhichang, Sun Jiemin, 1988. Analysis of hydrological and sediment conditions in Nanhui Nearshore of the Yangtze Estuary and its adjacent sea areas during flood season. In: Chen Jiyu, Shen Huanting, Yun Caixing (eds.). *Process of Dynamics and Geomorphology of the Changjiang Estuary*. Shanghai: Shanghai Scientific and Technical Publishers. (in Chinese)
- Li Jiufa, Wan Xinning, Ying Ming *et al.*, 2006. Study on formation and evolvment of Jiudian Shoal in the Changjiang Estuary. *Journal of Sediment Research*, (6): 44–49. (in Chinese)
- Miliman J D, Shen H T, Yang Z S *et al.*, 1985. Transport and depositon of River sediment in the Changjiang Estuary and adjacent continental shelf. *Continental Shelf Research*, 4: 37–45.

- Roberts W, Hir P L, Whitehouse R J S, 2000. Investigation using simple mathematical models of the effect of tidal currents and waves on the profile shape of intertidal mudflats. *Continental Shelf Research*, 20: 1079–1097.
- Shen Huanting, Zhang Chao, Mao Zhichang, 2000. Patterns of variations in the water and sediment fluxes from the Changjiang River to the estuary. *Oceanologia et Limnologia Sinica*, 31(3): 288–294. (in Chinese)
- Shepard F P, 1954. Nomenclature based on sand-silt-clay ratios. *Journal of Sedimentary Petrology*, 24: 151–158.
- Van Ledden M, 2003. Sand-mud segregation in estuaries and tidal basins [D]. the Netherlands: Delft University of Technology, 50pp.
- Wan Xinning, Li Jiufa, He Qing *et al.*, 2003. Water and sediment fluxes in the middle and lower Yangtze River. *Journal of Sediment Research*, (4): 29–35. (in Chinese)
- Winterwerp Johan C, van Kesteren Walther G M, 2004. Introduction to the physics of cohesive sediment in the marine environment. Published by Elsevier.
- Yan Hong, Dai Zhijun, Li Jiufa *et al.*, 2010. Distribution of surficial tidal flat sediments in the Yangtze Estuary. *Acta Geographica Sinica*, 2009(5): 629–637.
- Yan Yixin, Gao Jin, Zhu Yuliang *et al.*, 2001. Preliminary study on relationship between Deepwater Channel Regulation and riverbed evolution. *Journal of Hohai University*, 5: 7–12. (in Chinese)
- Yang Ou, Liu Cangyu, 2002. Analysis on sediment transport patterns sediment sources of North Branch of Changjiang Estuary. *Journal of Hydraulic Engineering*, (2): 79–84.
- Yang S L, Li H, Ysebaert T *et al.*, 2008. Spatial and temporal variations in sediment grain size in tidal wetlands, Yangtze Delta: On the role of physical and biotic controls. *Estuarine, Coastal and Shelf Science*, 77: 657–671.
- Yang Shilun, Zhao Qingying, Ding Pingxing *et al.*, 2001. Seasonal Changes in bed level of the passage in the mouth bar area of the Yangtze (Changjiang) River. *Resources and Environment in the Yangtze Basin*, 10(3): 258–265. (in Chinese)
- Yoshiki Saito, Yang Zuosheng, Hori Kazuaki, 2001. The Huanghe (Yellow River) and Changjiang (Yangtze River) deltas: A review on their characteristics, evolution and sediment discharge during the Holocene. *Geomorphology*, 41: 219–231.
- Zhang Hongsheng, 2002. Mathematical models of wave propagation in coastal region [D]. Shanghai: East China Normal University. (in Chinese)
- Zhu Huifang, Yun Caixing, Mao Zhichang *et al.*, 1988. The characteristics and empirical relationships of wind-wave of the Changjiang Estuary. In: Chen Jiyu, Shen Huanting, Yun Caixing (eds.). *Process of Dynamics and Geomorphology of the Changjiang Estuary*. Shanghai: Shanghai Scientific and Technical Publishers, 1988: 166–177. (in Chinese)